THE ASTRONOMICAL JOURNAL, 122:3407–3418, 2001 December
© 2001. The American Astronomical Society. All rights reserved. Printed in U.S.A.

SPATIALLY RESOLVED STIS SPECTRA OF WR + OB BINARIES WITH COLLIDING WINDS[1]

SÉBASTIEN LÉPINE,[2] DEBRA WALLACE,[3] MICHAEL M. SHARA,[2] ANTHONY F. J. MOFFAT,[4] AND VIRPI S. NIEMELA[5,6]

Received 2001 July 15; accepted 2001 September 20

ABSTRACT

We present spatially resolved spectra of the visual WR + OB massive binaries WR 86, WR 146, and WR 147, obtained with the Space Telescope Imaging Spectrograph on board the *Hubble Space Telescope*. The systems are classified as follows: WR 86 = WC 7 + B0 III, WR 146 = WC 6 + O8 I–IIf, WR 147 = WN 8 + O5–7 I–II(f). Both WR 146 and WR 147 are known to have strong nonthermal radio emission arising in a wind-wind collision shock zone between the WR and OB components. We find that the spectra of their O companions show Hα profiles in emission, indicative of large mass-loss rates and consistent with the colliding-wind model. Our spectra indicate that the B component in WR 86 has a low mass-loss rate, which possibly explains the fact that WR 86, despite being a long-period WR + OB binary, was not found to be a strong nonthermal radio emitter. Because of the small mass-loss rate of the B-star component in WR 86, the wind collision region must be closer to the B star and smaller in effective area, hence generating smaller amounts of nonthermal radio emission. Absolute magnitudes for all the stars are estimated based on the spectral types of the components (based on the tables by Schmidt-Kaler for OB stars and van der Hucht for WR stars) and compared with actual, observed magnitude differences. While the derived luminosities for the WC 7 and B0 III stars in WR 86 are consistent with the observed magnitude difference, we find a discrepancy of at least 1.5 mag between the observed luminosities of the components in each of WR 146 and WR 147 and the absolute magnitudes expected from their spectral types. In both cases, it looks as though either the WR components are about 2 mag too bright for their spectral types or that the O components are about 2 mag too faint. We discuss possible explanations for this apparent discrepancy.

Key words: binaries: visual — stars: early-type — stars: winds, outflows — stars: Wolf-Rayet

1. INTRODUCTION

OB stars (which as a group include stars of spectral type between O3 and B2) are the most massive main-sequence objects. They are generally found in young clusters and associations because their life spans are too short to carry them far from their birthplaces. Consequently, they are often subjected to considerable interstellar absorption. Wolf-Rayet (WR) stars are believed to be the evolved counterparts of at least some OB stars, and they mostly correspond to a phase where the massive star has lost all its external hydrogen envelope through stellar winds (Conti 1976). Wolf-Rayet stars generate intense stellar winds reaching rates of $\dot{M} \gtrsim 10^{-5}\ M_{\odot}\ \mathrm{yr}^{-1}$ and terminal speeds $v_{\infty} \gtrsim 10^{3}\ \mathrm{km\ s}^{-1}$. The Wolf-Rayet photosphere arises, not from the hydrostatic surface, but in the wind itself, which, besides He lines, is dominated either by ions of nitrogen (WN stars) or carbon and oxygen (WC stars). Hence the spectrum of a WR star is dominated by very broad lines of He and heavier elements.

Current estimates indicate that at least ~40% of WR stars are in multiple systems (Moffat 1995). The presence of a companion can be suspected from a composite spectrum showing OB absorption lines or from the apparent "dilution" of the WR emission lines by extra continuum emission (Smith, Shara, & Moffat 1996). Confirmation of multiplicity is usually based on radial velocity studies. Indirect confirmation can also be made by the detection of colliding-wind effects (e.g., Tuthill, Monnier, & Danchi 1999; Williams 1999). A small number of OB companions in very long period ($P > 50$ yr) systems have also been found from speckle interferometry or direct imaging (Hartkopf et al. 1993; Williams et al. 1997; Niemela et al. 1998). These systems are particularly interesting because the absolute magnitude of the WR component can be directly inferred from that of its companion, assuming the two stars are at the same distance.

In the IR and radio regimes, WR stars are dominated by thermal, free-free emission from the dense, expanding envelope. However, ≈40% of WR stars have been observed to have a radio spectral energy distribution consistent with nonthermal emission associated with synchrotron radiation and high-energy phenomena. Eichler & Usov (1993) have demonstrated how nonthermal radio emission could arise from the collision between the outflows from two early-type stars in a binary system. As it turns out, binary systems are overrepresented in the sample of nonthermal emitters, which prompted van der Hucht (1992) to suggest that all nonthermal WR emitters were actually in binary systems, with the wind collision being responsible for the nonthermal emission.

[1] Based on observations with the NASA/ESA *Hubble Space Telescope*, obtained at the Space Telescope Science Institute, which is operated by the Association of Universities for Research in Astronomy, Inc., under NASA contract NAS 5-26555.

[2] Department of Astrophysics, Division of Physical Sciences, American Museum of Natural History, Central Park West at 79th Street, New York, NY 10024; lepine@amnh.org, mshara@amnh.org.

[3] Department of Physics and Astronomy, Georgia State University, Atlanta, GA 30303; wallace@chara.gsu.edu.

[4] Département de Physique, Université de Montréal, C.P. 6128 Succursale Centre-Ville, Montréal, Québec H3C 3J7, Canada; moffat@astro.umontreal.ca.

[5] Facultad de Ciencias Astronómicas y Geofisicas, Universidad Nacional de La Plata, Paseo del Bosque s/n, 1900 La Plata, Argentina; virpi@fcaglp.unlp.edu.ar.

[6] Member of Carrera del Investigador, CIC-BA, Argentina.

The colliding-wind model has been strikingly confirmed by radio observations of two nonthermal WR emitters (Williams et al. 1997; Dougherty et al. 1996) confirmed to be in binary systems with OB companions (Niemela et al. 1998). The nonthermal emission is found to be associated with a distinct region whose photocenter is located *on or close to the line joining the WR star and its OB companion*, the WR star itself being associated with a thermal source. However, not all WR + OB binaries are found to be nonthermal emitters. Dougherty & Williams (2000) have noted that WR + OB systems form two distinct groups, with most thermal emitters being in short-period systems, while the nonthermal emitters are all in long-period systems with large component separation. Since the nonthermal emission arises locally, at the wind-wind collision front, one might expect to observe nonthermal radio emission only from widely separated WR + OB binaries, whose large collision fronts are expected to be located well outside the extended radio photosphere of the WR wind. In short-period binaries the collision front occurs much deeper in the wind of the WR star, in which case nonthermal radio emission is not expected to be observed as the collision front lies inside the WR radio photosphere.

More recently, the conjecture that all nonthermal emitters are colliding-wind binaries has been put in doubt by Wallace et al. (2000), who have failed to identify companions for eight WR stars with nonthermal radio emission down to a mean projected separation of ≈ 20 AU. Since this scale is within the distance of the radio photosphere, either nonthermal radio emission in these stars arises farther out in the wind itself (possibly generated by intrawind shocks), or nonthermal radio emission does arise in colliding winds, but the radio photosphere is much smaller than predicted. If the latter hypothesis is correct though, all the apparently single nonthermal radio emitters should have companions on close orbits and should have been identified as spectroscopic binaries. The single-star explanation remains to be confirmed.

The colliding-wind model, however, is successful in explaining nonthermal emission in long-period WR + OB systems. But are all long-period systems nonthermal emitters? So far, there is one exception to the rule: the long-period WR + OB system WR 86. However, while WR 86 is not strictly defined as a nonthermal emitter, its spectral index is consistent with a "composite" thermal/nonthermal source; i.e., it is consistent with weak nonthermal emission (Dougherty & Williams 2000).

This paper presents spatially resolved STIS spectra of the components in the visual WR + OB systems WR 86, WR 146, and WR 147. The observations and data reduction are discussed in § 2. Spectral classification of the components is presented in § 3. This allows us to estimate both the absolute luminosity of the components and the mass-loss rates of the OB stars. Results are discussed in the light of the colliding-wind model in § 4. We briefly summarize our findings in § 5.

2. OBSERVATIONS

Long-slit spectroscopy of the stars WR 86, WR 146, and WR 147 has been obtained with the STIS spectrograph on board the *Hubble Space Telescope*. In each case, observations were carried out with the slit length oriented as close as possible to the apparent position angle of the binaries. Niemela et al. (1998) have estimated the position angles to be P.A. = 109° ± 9°, 21° ± 4°, and 350° ± 2° for WR 86, WR 146, and WR 147, respectively. The exact orientation of the STIS slit depends on the orientation of *HST* at the time of the observation; hence the above P.A.'s were used as scheduling constraints. Observations were finally carried out with P.A. = 106°.1, 18°.8, and 360°.2, for WR 86, WR 146, and WR 147, respectively. In each case, the orientation was such that the brightest component in the V band appeared on the larger CCD column number. The width of the $52 \times 0''.5$ slit is on the order of or larger than the separation between the components; hence the small difference ($<13°$) between the orientation angle at the time of observation and the P.A.'s of the systems has negligible effects on the throughput.

The two stars in the WR 147 system are clearly resolved by STIS; we used standard IRAF aperture extraction to obtain their spectra. On the other hand, the relatively broad wings in the STIS point-spread function (PSF) resulted in the WR 86 and WR 146 spectra being resolved, but with significant blending (Fig. 1). To complicate matters, the shape of the PSF was found to be dependent on the wavelength to a level that significantly affects the spectral extraction of barely resolved sources such as those from WR 86 and WR 146 (but is of little consequence for clearly resolved sources such as in WR 147). We performed a multidimensional fit for each column on the CCD to extract a blended double profile $G(y)$ with the general shape[7]

$$G(y) = A1 \exp -\left[\frac{(y - y1)^2}{2\sigma^2}\right]^k + A2 \exp -\left[\frac{(y - y2)^2}{2\sigma^2}\right]^k , \quad (1)$$

where $y1$ and $y2$ are the spatial locations of the stars along a column, and A1 and A2 are the amplitudes of the profiles for each star. The shape of the stellar profiles is governed by the dispersion parameter σ and the "peakiness" parameter k (which sets the relative strength of the PSF wings). Because the mean dispersion σ of the PSF is found to be close to the pixel size, we resampled the profile over individual pixels y_i from the continuous function $G(y)$ using

$$G'(y_i) = \int_{y_i - 0.5}^{y_i + 0.5} G(y)dy , \quad (2)$$

where y_i are integers representing the CCD lines.

We then used the assumption that the separation between the stars should be constant and independent of the wavelength. To determine the separation between the stars, we first performed a fit of $G'(y_i)$ in the six-dimensional parameter space ($y1$, $y2$, σ, k, A1, A2) and calculated the separation Δy between the stars from the mean values of $y2 - y1$ obtained from each CCD column. We then fixed $y2 = y1 + \Delta y$ and performed a second (more robust) fit in the five-dimensional space ($y1$, σ, k, A1, A2) for each CCD column.

Using the derived values for Δy and the STIS pixel size of $0''.0507$ pixel^{-1}, we estimate the separation along the slit between the components of WR 86, WR 146, and WR 147

[7] The profile described by equation (1) is not a Gaussian, although is does assumes the Gaussian form for the special case $k = 2$. We used this form for its simplicity and stability under the multidimensional fit. We did attempt to use other simple mathematical forms to describe the PSF, e.g., Moffat (1969) functions, only to obtain equivalent results in the spectral extraction.

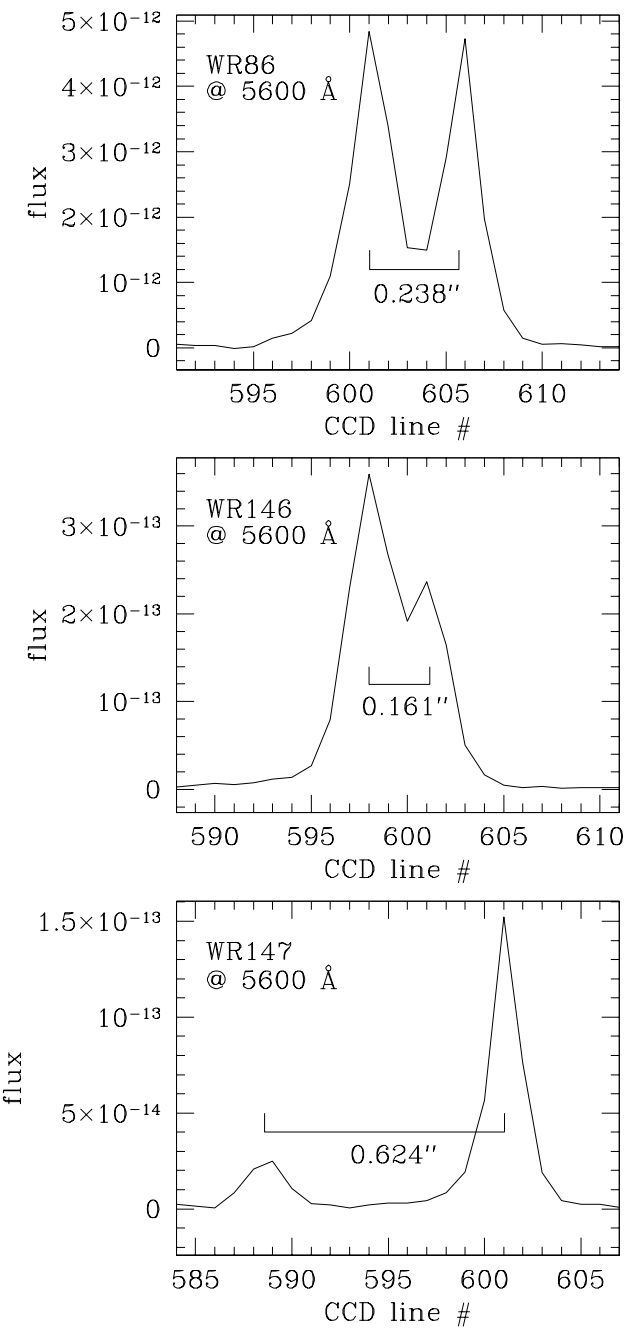

FIG. 1.—Resolution of the WR + O systems along the slit of the STIS camera at 5600 Å. The slit is oriented along the line joining the stars, with the OB star to the left and the WR star to the right on this figure.

to be $0''.239 \pm 0''.006$, $0.161 \pm 0''.005$, and $0''.624 \pm 0''.015$, respectively. The P.A. of the slit was always within 13° of the line joining the two stars; hence these values should be reliable estimates of the component separations. Our values for WR 146 and WR 147 are consistent with the separation calculated from the WFPC2 image by Niemela et al. (1998). For WR 86, our derived separation is outside of 1 σ of the $0''.286 \pm 0''.039$ range derived by Niemela et al., but well within the $0''.230 \pm 0''.013$ range cited in the *Hipparcos* catalog.

Results of the multidimensional fits confirm the existence of a systematic variation in the PSF pattern with wavelength (Fig. 2). The pattern also differs between WR 86 and WR 146, despite the same spectral coverage, which suggests that the shape of the PSF also depends on where the source falls along the slit (the WR 86 and WR 146 systems have been recorded on slightly different CCD columns). This raises the possibility that the PSF may be slightly different for each component in any one system, which may result in some inaccuracies in the spectral extraction.

The two stellar components in both WR 86 and WR 146 were apparently separated reasonably well across most of the spectral range. The only exception occurs at wavelengths close to the very bright WR emission line C IV λ5808 (at which point the WR star is significantly brighter than the OB star), where a small contamination of the WR flux onto the OB companion spectrum apparently occurred. This is clearly due to an imperfect PSF model. In particular, the wings of the PSF showed evidence for a weak diffraction pattern, which our model does not reproduce. This results in some contamination of one spectrum by some light from the other component. However, this contamination is apparent only for the broad C IV emission line, because of the large difference in the brightness of the WR and OB components at that wavelength, and is negligible elsewhere (below instrumental noise levels). Fortunately, this contaminated C IV emission from the WR component can be unambiguously identified in the OB star spectra, whose spectrum does not normally exhibit such a broad emission feature at that wavelength. Because the spectra are generally well separated and because contamination effects are relatively small, we did not attempt to refine the PSF model further, which would have required the use of extra parameters and would have made the multidimensional fit much more difficult to perform.

The resolved spectra for all three stars are shown in Figure 3. It turns out that the brightest component in the V band in each pair is the Wolf-Rayet star, even though the continuum emission from the OB star is actually larger in WR 86 and WR 146 (the WR stars in these systems are brighter in V because of their strong emission lines). Contamination of the OB spectra by the very bright C IV λ5812 line is very obvious in WR 146 (see Fig. 5). Examination of the C IV λ5812 contamination profile in the spectrum of the O component shows that contamination becomes apparent as the monochromatic intensity from the WR star reaches $\approx$3 times that of the O companion. Since the relative WR intensity is below that level over the remainder of the spectrum, we conclude that contamination effects must be negligible over the remainder of the spectral range. Hence, any feature observed elsewhere in the spectrum of the O star is assumed to be intrinsic. In WR 86, the components are further apart; hence the extracted spectra are less susceptible to contamination effects. Our extracted spectra of WR 86 show evidence for a weak contamination of the CIVλ5812 line and also possibly from C III λ5696 (see Fig. 7). Both WR lines have monochromatic intensity reaching $\approx$3 times that of the B-star continuum. Because these lines are the brightest features in the WR component of WR 86, and because they yield only weak contamination effects, we conclude that no other WR features contaminates the B spectrum significantly, and any other feature observed in the B-star spectrum must be intrinsic.

In each system, the slopes of the continua from the WR stars and the OB companions, as well as the strength of the interstellar absorption lines, are all consistent with equal

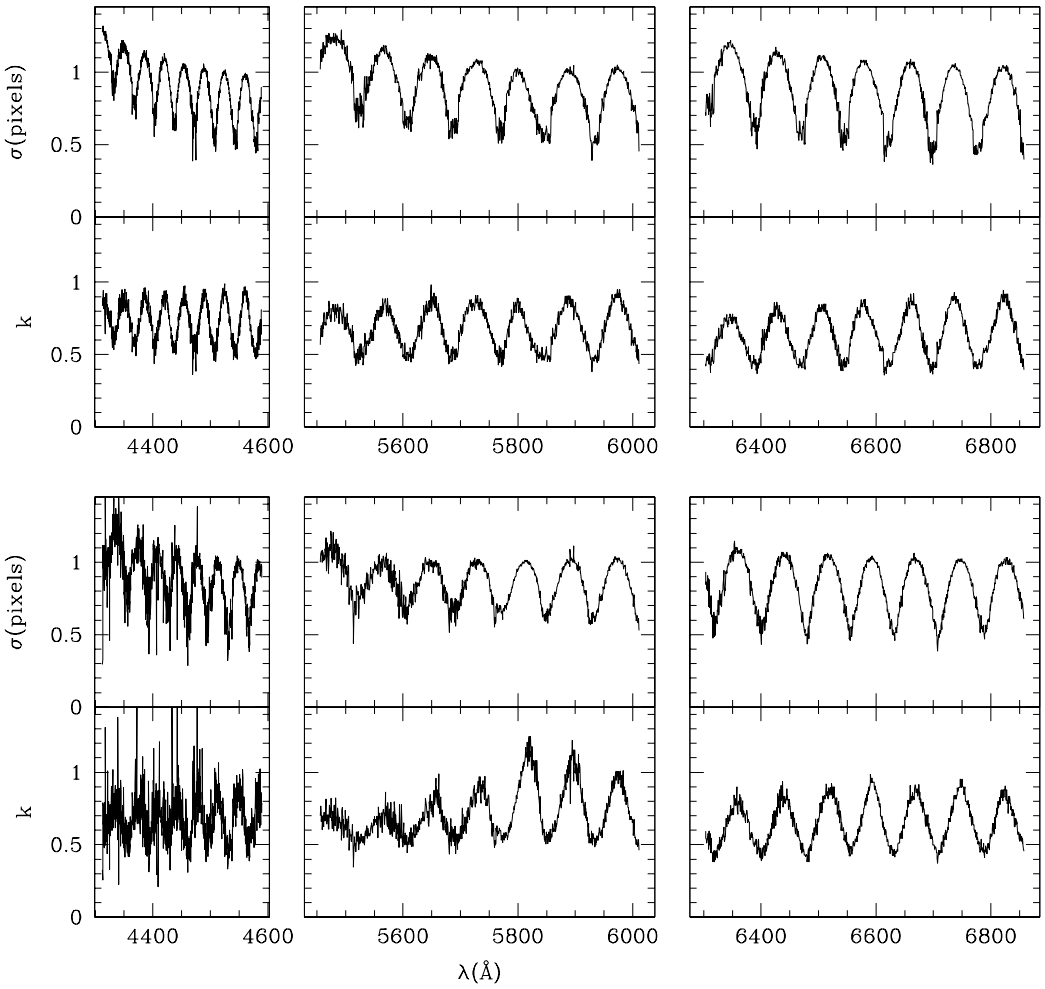

FIG. 2.—Dispersion parameter σ and "peakiness" parameter k of the stellar profiles measured for the WR 86 (*top*) and WR 146 (*bottom*) systems. Values are derived from a double-profile multidimensional fit at each column on the STIS CCD image. The point-spread function is clearly dependent on the wavelength; patterns also differ significantly between systems. The fit also yields deblended spectra of the individual components (Figs. 3–6). Deblending is reasonably good, except at wavelengths where the WR star becomes $\gtrsim 3$ times brighter than the O star, at which point this model is not accurate enough to yield reliable deblended spectra (see text).

amounts of reddening. This supports the idea that the components in each system are approximately at the same distance and most likely to be physically related. In both WR 146 and WR 147, we confirm that the WR (O) component is to the south (north), consistent with the colliding-wind interpretation of their radio maps (see Niemela et al. 1998). For WR 86, the WR component is to the northwest and the B component to the southeast.

We did not find any trace of background or "nebular" emission in the long-slit spectral images within the instrumental limits. Attempts have been made to extract spectra at different locations along the slit, but only the wings of the PSF from the stellar components and other instrumental features were detected. This lack of detection is significant for WR 146 and WR 147, which are known to be colliding-wind binaries. If there is any diffuse emission in the optical associated with the colliding-wind region, we estimate that it must be weaker than 5×10^{-15} ergs cm^{-2} s^{-1} Å^{-1} arcsec^{-1}.

Line identifications for each of the WR and OB star components are listed in Tables 1–6. The resolution of the STIS spectra was ≈ 1.4 Å, which is the accuracy in the central wavelength measurements. Estimated errors on equivalent width measurements W_λ are listed individually. The error on W_λ depends on the strength of the line and on whether it was resolved or in a blend. We do not give the mean central wavelengths of the lines in the WR stars, because the very broad profiles make the central wavelengths very unreliable for line identification. Most of the bright WR lines are actually blends of several different lines; the line identification and rest wavelength given in the tables is for the transition which most probably contributes to the largest part of the line emission.

3. SPECTRAL CLASSIFICATION

3.1. *WR 86*

This is the $V = 9$th magnitude system HD 156327, located at $\alpha = 17^{\rm h}18^{\rm m}23^{\rm s}.06$, $\delta = -34°24'30''.6$ (J2000.0). It was initially listed as a Wolf-Rayet binary with spectral type WC 7 + B0 V (Roberts 1962; Smith 1968) based on the presence of H and He I absorption lines in the blue. It was included in the Sixth Catalog of Galactic Wolf-Rayet stars (van der Hucht et al. 1981) under the designation WR 86 and given a WC 7 + abs spectral type, implying that absorption lines could be intrinsic to the WR star, thus

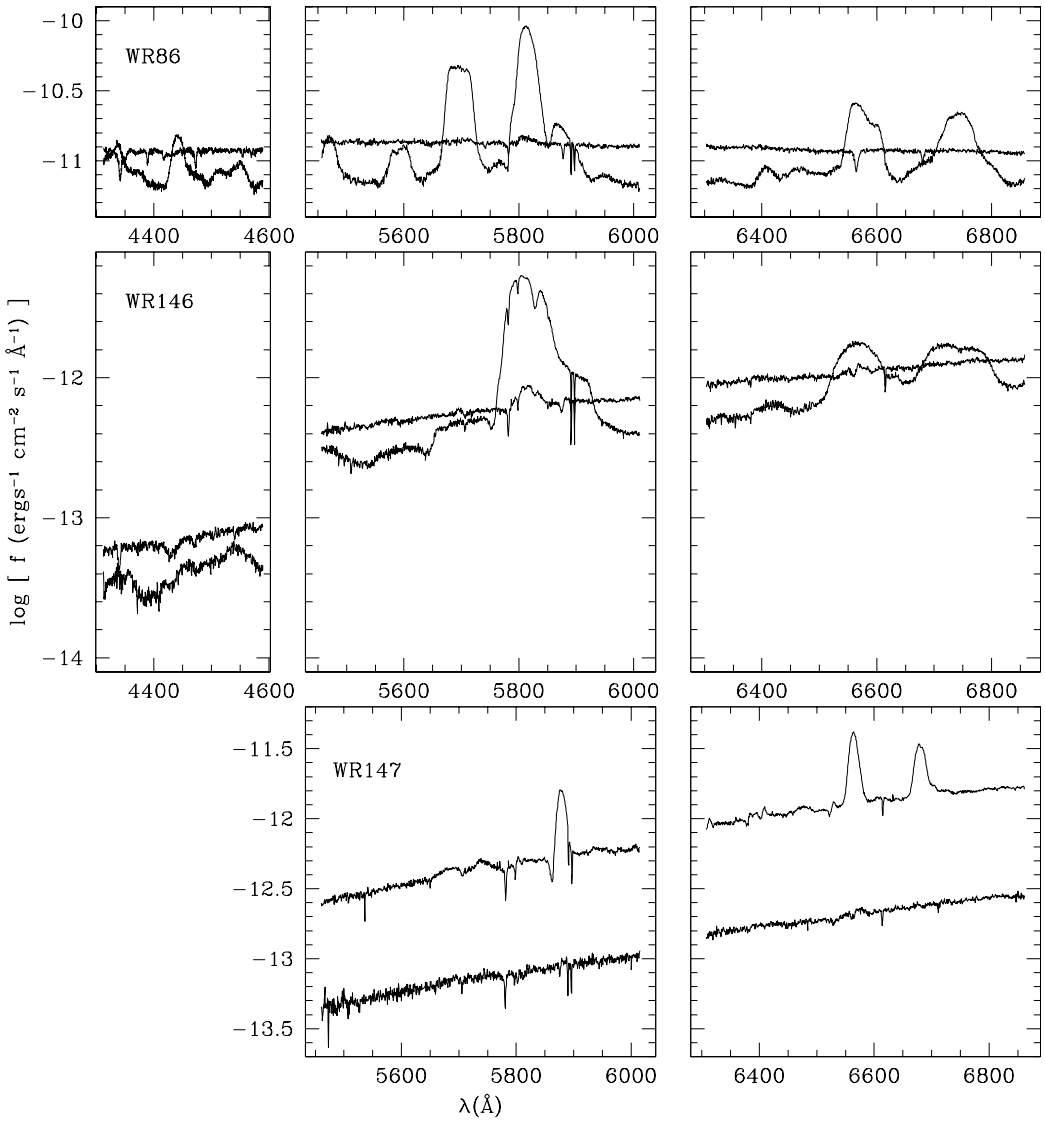

FIG. 3.—Resolved STIS spectra of the WR 86, WR 146, and WR 147 systems (*top to bottom*, respectively). Contamination of the OB spectrum by the brightest of the WR star features occurred in WR 86 and in WR 146 (C IV λ5812 emission line) because the stars were only separated by $\approx$2 standard deviations of the STIS point-spread function. Note the similar amounts of reddening and equivalent strengths of the interstellar absorption features for the pairs of stars in each system. Line identification is provided in Figs. 4–9.

questioning its double star status. However, HD 156327 was known to be a close visual double with separation $\rho \sim 0\farcs2$ (Jeffers, van de Bos, & Greeby 1963). The fact that Massey et al. (1981) failed to measure any radial velocity variation ruled out the idea of a *close* OB companion, strongly suggesting that the OB spectrum is associated with the visual companion (see Moffat et al. 1986). In any case, the star continued to be referred to as a WC 7 + abs throughout the 1980s.

The double star status was confirmed with speckle observations by Hartkopf et al. (1993), who resolved the star into two components with a $0\farcs237$ separation. The components were also clearly resolved by the WFPC2 camera on board *HST* (Niemela et al. 1998). Based on scanned image tube spectra of the pair, Niemela et al. suggested the companion to be a B0 star (detection of O II, Si III, and Si IV) with a luminosity class between I and III. The system is now listed in the seventh catalog of Wolf-Rayet stars (van der Hucht 2001) as "WC 7 (+ B0 III–I)."

Our STIS spectra confirm that the WR component is of subtype WC 7 (Fig. 4, with line equivalent widths listed in Table 1). The ratio of the equivalent widths of the C IV λ5801 and C III λ5696 lines is $\log W_\lambda$(C IV 5801)/$\log W_\lambda$(C III 5696) $\simeq$ 0.16, which is consistent with subtype WC 7 in the quantitative classification system of Crowther, De Marco, & Barlow (1998).

For the O component (Fig. 5; Table 2), our spectra confirm the B0 type, based on a comparison of the blue spectrum with the atlas of Walborn & Fitzpatrick (1990). We attempt to better constrain the luminosity class based on the strength of the Hγ absorption line, for which a calibration with the absolute magnitude has been derived by Millward & Walker (1985). We measure $W(\mathrm{H}\gamma) = 2.60 \pm 0.15$ Å, the uncertainty being largely attributable to the blend with O II λ4349. Following the Millward & Walker calibration, this corresponds to an absolute magnitude $M_V \simeq -4.8 \pm 0.2$. According to the B-star absolute magnitude calibration of Schmidt-Kaler

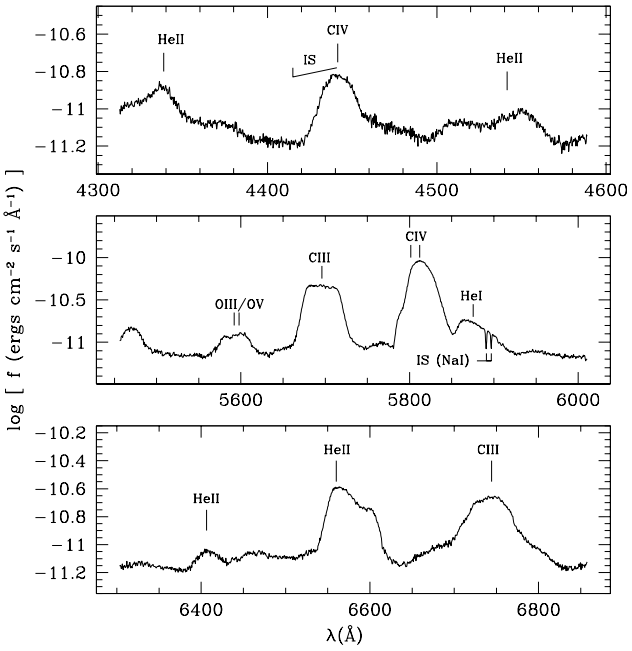

FIG. 4.—Line identification for the WR star component in the WR 86 system. Because emission lines are very broad, most of the features identified here are actually blends of several different lines. The identification is for the main contributor to each feature. Equivalent widths are listed in Table 1.

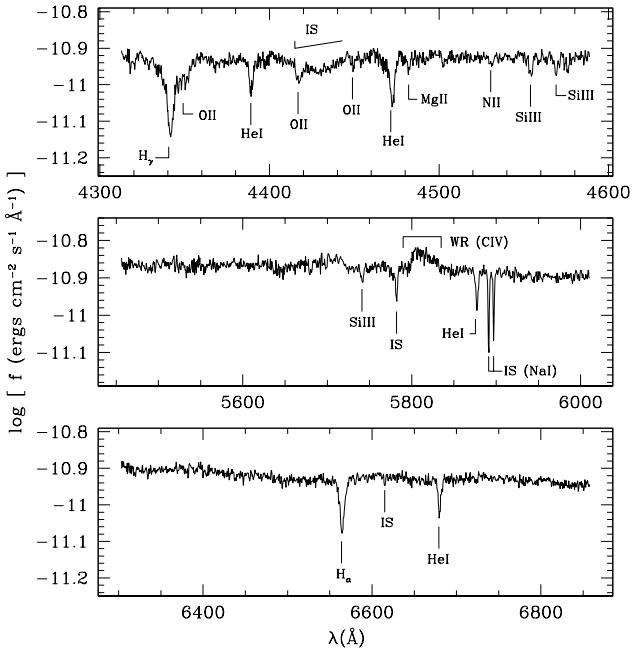

FIG. 5.—Line identification for the B star component in the WR 86 system. Contamination from the WR star is noted, along with the principal interstellar absorption features. Equivalent widths are listed in Table 2. The feature noted "WR (C IV)" is an instrumental contamination of the light from the WR component.

TABLE 1

LINE IDENTIFICATIONS IN THE SPECTRUM OF THE WR COMPONENT OF WR 86

ID	λ_{lab} (Å)	W_λ (Å)
He II.....	4338.7	-25.0 ± 5.0
C IV	4441.5	-31.9 ± 0.5
He II.....	4541.6	-15.0 ± 5.0
O III/O V.....	5592.2/5597.9	-31.8 ± 2.0
C III	5695.9	$-205. \pm 15.$
C IV	5801.3/5812.0	$-295. \pm 15.$
He I	5875.6	-50.0 ± 5.0
He II.....	6406.4	-13.0 ± 3.0
He II.....	6560.0	$-85.0 \pm 10.$
C III	6744.4	$-120. \pm 10.$

TABLE 2

LINE IDENTIFICATIONS IN THE SPECTRUM OF THE OB COMPONENT OF WR 86

ID	λ_{lab} (Å)	λ_{obs} (Å)	W_λ (Å)
H_γ	4340.5	4341.7	2.30 ± 0.20
O II.....	4349.4	4349.0	0.70 ± 0.20
He I	4387.9	4389.2	0.55 ± 0.05
O II.....	4414.9	4417.3	0.35 ± 0.05
O II.....	4448.3	4449.3	0.20 ± 0.05
He I	4471.5	4472.4	1.00 ± 0.10
Mg III	4479.0	4482.1	0.15 ± 0.05
N II.....	4530.4	4530.7	0.15 ± 0.05
Si III	4553.9	4554.2	0.35 ± 0.05
Si III	4567.8	4569.1	0.30 ± 0.05
Si III	5739.7	5741.6	0.30 ± 0.05
He I	5875.6	5877.2	0.70 ± 0.05
Hα.....	6561.9	6564.8	2.00 ± 0.05
He I/He II.....	6678.1/6683.2	6679.8	0.80 ± 0.05

(1982, hereafter SK82), this makes the star a B0 giant of class III. Since the WFPC2 photometry shows the two stars to have the same M_V (within the ± 0.09 observational errors), then the WR component is also estimated to have $M_V \simeq -4.8 \pm 0.2$. This value is largely consistent with the range of values quoted by van der Hucht (2001) for WC 7 stars.

Luminosity classes of early-B stars can also be estimated from the ratio of Si III λ5740 and He I λ5876. Comparison with the yellow-red atlas of Walborn (1980) shows the spectrum to be generally consistent with luminosity class III. While we can definitely rule out a class I for this object, it is not possible to rule out spectral class II on the basis of the Si III λ5740/He I λ5876 ratio. However, because the Hα line shows no trace of overlying wind emission (which occurs in most early-B stars with luminosity class I–II), we classify this system as WC 7 + B0 III.

3.2. *WR 146*

This star, located at $\alpha = 20^h35^m47^s.09$, $\delta = +41°22'44''.7$ (J2000.0), was initially classified as WC 6 by Roberts (1962) and as WC 5 by Smith (1968). It was listed as a WC 4 in the Sixth Catalog of Galactic Wolf-Rayet Stars (van der Hucht et al. 1981). Improved measurements of the line ratios led Smith, Shara, & Moffat (1990) to reclassify the WR star as WC 6.

Dougherty et al. (1996) observed the star at 1.6 and 2.5 GHz with the MERLIN array and resolved the source into two components, a thermal source and a nonthermal source, separated by 116 ± 14 mas. They attributed the thermal source to the WR star and the nonthermal source to a colliding-wind region between the WR star and an OB companion. Dougherty et al. (1996) also found weak hydrogen absorption lines (Hδ, Hγ) in an unresolved

blue spectrum of WR 146, which they attributed to the unresolved companion.

Optical WFPC2 images from *HST* clearly resolved the object into two components separated by $168'' \pm 31''$ and with very similar colors (Niemela et al. 1998). An overlap of the optical images and radio maps showed the nonthermal source to be located between the optical components, confirming the colliding-wind binary hypothesis. Assuming that the relative location of the nonthermal source matches the head of the bow shock, it is possible to calculate the ratio of the wind momentum fluxes. For WR 146, Niemela et al. obtained a ratio $\eta \equiv (\dot{M}v_\infty)_{\rm OB}/(\dot{M}v_\infty)_{\rm WR} \sim 0.1$. Given the large mass-loss rate expected from the WC 6 star, this requires the companion to have a relatively large mass-loss rate also. Based on the momentum ratio and on the relative colors of the components, Niemela et al. suggested the companion to be O6–O5 V–III.

More recently, Dougherty, Williams, & Pollacco (2000) obtained a 3800–4500 Å spectrum of WR 146 at the 4 m William Herschel Telescope (WHT). Though blended with emission lines from the WR star, the relatively narrow absorption lines from the O companion were clearly identified. Their λ4541 He II/λ4471 He I equivalent width ratio (the principal diagnostic of the O-type sequence) indicated a spectral type O8. Though several features were also suggestive of a high luminosity class, they did not assign a luminosity class due to a lack of the main luminosity diagnostic lines in their spectrum. The system is now listed as WC 6 + O8 in the seventh catalog of Wolf-Rayet stars (van der Hucht 2001).

Our STIS spectra of the WR component (Fig. 6; Table 3) confirms the WC 6 classification. We measure a line equivalent width ratio $\log W_\lambda$(C IV 5801)/$\log W_\lambda$(C III 5696) $\simeq$ 1.03, consistent with subtype WC 6 in the quantitative classification system of Crowther et al. (1998). The lines in this star are especially broad, indicating a large wind terminal

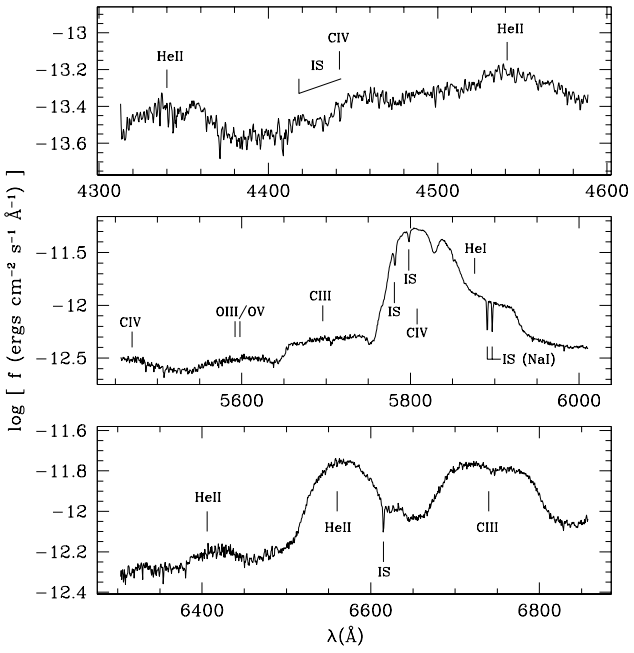

FIG. 6.—Line identification for the WR star component in the WR 146 system. Because emission lines are very broad, most of the features identified here are actually blends of several different lines. The identification is for the main contributor to each feature. Equivalent widths are listed in Table 3.

TABLE 3

LINE IDENTIFICATIONS IN THE SPECTRUM OF THE WR COMPONENT OF WR 146

ID	$\lambda_{\rm lab}$ (Å)	W_λ (Å)
O III/O V.....	5592.2/5597.9	-22.0 ± 3.0
C III	5695.9	-55.0 ± 8.0
C IV	5801.3/5812.0	$-600. \pm 35.$
He I	5875.6	$-140. \pm 35.$
He II.....	6406.4	-15.0 ± 3.0
He II.....	6560.0	$-165. \pm 10.$
C III	6744.4	$-200. \pm 15.$

velocity ($v_\infty \simeq 2900$ km s^{-1} as measured by Eenens & Williams 1994).

For the OB component (Fig. 7; Table 4) we measure a line ratio He II λ4541/He I λ4471 = 0.39, which is consistent with a spectral type O9 in the system of Conti & Alschuler

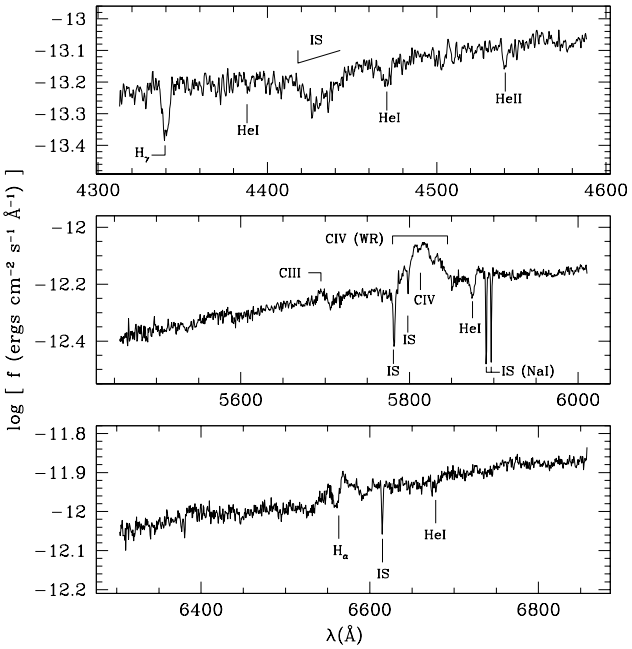

FIG. 7.—Line identification for the O-star component in the WR 146 system. Contamination from the WR star is noted, along with the principal interstellar absorption features. Equivalent widths are listed in Table 4. The feature noted "C IV (WR)" is an instrumental contamination of the light from the WR component.

TABLE 4

LINE IDENTIFICATIONS IN THE SPECTRUM OF THE OB COMPONENT OF WR 146

ID	$\lambda_{\rm lab}$ (Å)	$\lambda_{\rm obs}$ (Å)	W_λ (Å)
Hγ	4340.5	4339.6	1.50 ± 0.10
He I	4387.9	4388.7	0.20 ± 0.05
He I	4471.5	4470.0	0.80 ± 0.05
He II	4541.5	4540.3	0.40 ± 0.05
C III	5695.9	5695.1	-0.65 ± 0.05
C IV	5811.9	5811.2	0.22 ± 0.05
He I	5875.6	5874.8	1.0 ± 0.10
Hα.....	6561.9	6568.3	-4.85 ± 0.25
He I/He II.....	6678.1/6683.2	6678.3	0.15 ± 0.05

(1971) and Conti (1973). The He I λ4471 line does look significantly broader than He II, which may be due to noise but could also result from blending of the He I λ4471 with some other unidentified line. On close examination, the He I λ4471 profile in the B0 III component of WR 86 does look asymmetric, with the blue side of the line being unusually extended. If this is due to some unidentified IS absorption feature (we do indeed see a shallow absorption trough at the same wavelength in the WR spectrum, which could also be the signature of this IS feature; see Fig. 6), then the EW of this line is most likely to be overestimated in WR 146. We consider the He I λ4388 line, and note that it is clearly weaker than He II λ4540; the spectral atlas of Walborn & Fitzpatrick (1990) shows that this generally does not occur in O9 type stars where both lines have about the same EW. It is, however, consistent with spectral type O8, and we thus also adopt this classification for the O star in WR 146.

The main luminosity diagnostic for O8–O9 stars is the increase in the strength of the Si IV $\lambda\lambda$4089, 4116 at higher luminosities and the change in N III $\lambda\lambda$4634, 4640 and He II λ4686 from absorption to emission (Walborn & Fitzpatrick 1990). While the WHT spectrum of Dougherty et al. included both Si IV lines, they were found to be blended with the Hδ line. Unfortunately, neither the STIS nor the WHT spectrum covers the He II λ4686 region. However, we note the presence of a weak emission feature centered on λ5696 which we attribute to C III line emission. Both the C III λ5696 and Hα lines have been shown by Walborn (1980) to behave like N III $\lambda\lambda$ 4634, 4640 and He II λ4686, respectively.

The Hα profile in the O star component shows a narrow but relatively shallow absorption trough flanked by relatively broad wings. The Hα line in the O star is coincident with the He II λ6560 complex in the Wolf-Rayet star, which raises the possibility of contamination into the O spectrum, which would explain the broad wings. However, we argue that the broad Hα emission profile is intrinsic to the O star: (1) the intensity of the He II λ6560 complex relative to the O star continuum is comparable to that of the broad shoulder in the C IV λ5812 complex (between $\lambda\lambda$5850 and 5950), and we see no obvious contamination of the O star spectrum by the latter; (2) the Hα profile in the B0 component in WR 86 does not show any broad wings, while it was more prone to being contaminated by the more intense He II λ6560 complex from its WR component; (3) the centroid of the Hα absorption trough is 6.4 Å larger than the measured lab value, which suggests that the central trough is being distorted as the line is filled up with Hα in emission, and (4) the overall shape of the Hα profile is very similar to that of other OIf stars (e.g., Cygnus OB No. 7 and HD 210839; see Fig. 6 in Herrero, Puls, & Villamariz 2000), including both the central narrow absorption and the broad emission wings.

The behavior of C III λ5696 and Hα in the O component of WR 146 clearly rules out any luminosity class fainter than II. Because the Hα line is not found to be strongly in emission, as in O8 I stars, a spectral type O8 II is the most reasonable classification. A secondary indicator for the luminosity class is the ratio He I λ4388 / He I λ4471, which correlates with the mass-loss rate. Our spectrum yields He I λ4388/He I λ4471 = 0.2, which suggests that the star is Of. The weakness of Hγ ($W_\lambda = 1.5$) is also consistent with large intrinsic luminosity; the Millward & Walker (1985) relationship suggests $M_V \gtrsim -6$ which, for O8, is consistent with luminosity class I–II (SK82). From these lines of evidence, we classify this system as WC 6 + O8 I–IIf.

3.3. *WR 147*

This star, located at $\alpha = 20^h36^m43^s.65$, $\delta = +40°21'07''.3$ (J2000.0), was resolved into a double radio source with a thermal lobe and a nonthermal lobe by Churchwell et al. (1992). Williams (1995) hypothesized that the nonthermal lobe was the result of a colliding-wind interaction with an unseen companion. The companion was first identified as a faint component in an IR image of WR 147 (Williams et al. 1997), and confirmed in the optical by *HST* WFPC2 observations (Niemela et al. 1998). Based on the relative K magnitude between the WN 8 star and the IR companion ($K_{OB} - K_{WR} = 3.04 \pm 0.09$), and, assuming the WN 8 star to have an absolute magnitude $M_K \approx -6$, Williams et al. claimed the OB companion to be consistent with a spectral type B0.5 V. In the optical the magnitude difference between the two components is observed to be $V_{OB} - V_{WR} = 2.16 \pm 0.09$, which is too small for a B0.5 V companion, and Niemela et al. (1998) proposed that the star is of earlier type.

Our STIS data for the WR component in WR 147 (Fig. 8; Table 5) show a spectrum typical of a WN 8 star, with a relatively strong P Cygni profile in He I λ5876. Also present are the weak He II $\lambda\lambda$6311, 6406, and 6527 lines—all with P Cygni profiles. Weak N II $\lambda\lambda$5680, 5686 lines are also detected, consistent with a late-type WN star.

Our WR 147 spectrum in the blue regime is of very poor quality and is not shown in this paper. Because of the considerable interstellar reddening, the WR 147 system is several magnitudes fainter in the blue, and our *HST* STIS exposures were not programmed appropriately for this relatively faint target. Hence it is not possible to obtain a precise, reliable spectral type for the O component, since classification of OB stars is largely based of the ratio of He I and He II lines in the blue. However, our spectrum shows a very weak He I λ5876 line, while He I λ6678 is too weak to even be detected (Fig. 9, Table 6). Since He I is very strong in late-O stars and early-B stars (type B2 being where He I reaches a maximum; see Walborn & Fitzpatrick 1990), this suggests that this star is either earlier than O8 or mid–late B. Because He becomes

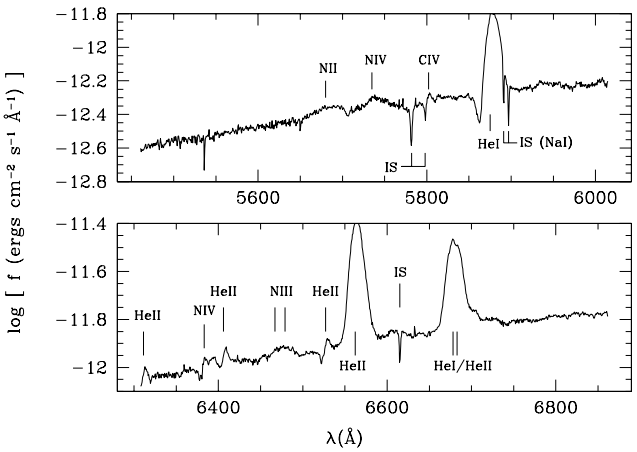

FIG. 8.—Line identification for the WR star component in the WR 147 system. Because emission lines are very broad, most of the features identified here are actually blends of several different lines. The identification is for the main contributor to each feature. Equivalent widths are listed in Table 5.

TABLE 5

LINE IDENTIFICATIONS IN THE SPECTRUM OF THE WR COMPONENT OF WR 147

ID	λ_{lab} (Å)	W_λ (Å)
N II.....	5679.6	-6.0 ± 1.0
N IV.....	5736.9	-5.8 ± 1.0
C IV.....	5801.3/5812.0	-0.8 ± 0.2
He I.....	5875.6	-35.0 ± 1.0
He II.....	6310.8	-0.6 ± 0.2
N IV.....	6380.7	-0.8 ± 0.2
He II.....	6406.4	-0.9 ± 0.2
N III.....	6467.0/6478.7	-3.2 ± 0.3
He II.....	6527.1	-1.0 ± 0.1
He II.....	6560.0	-45.0 ± 1.5
He I/He II.....	6678.1/6683.2	-30.0 ± 1.5

doubly ionized in early-O stars, we can also exclude a spectral type earlier than O5. Furthermore, the presence of high-ionization C IV lines unambiguously rules out any spectral type B or later. These lines of evidence suggests that our star can only be in the range O5–O7. An O5–O7 spectral type is consistent with the relatively strong C IV $\lambda\lambda$5801, 5812 lines, which are strongest in this spectral range (Walborn 1980). Because we lack a clear line ratio and because there is considerable scatter among O stars in the equivalent widths of single species, it is, however, not possible to constrain the spectral type further. Due to the lack of other objective classification criteria, the O5–O7 assignment must be regarded as tentative.

The Hα region shows a very shallow absorption trough, flanked by broad emission wings, very similar to the profile observed in the O8 component in WR 146. The broad emission wings cannot be explained by contamination from the WN 8 star, since the two components are well resolved by STIS and any (very weak) component arising in the very broad wing of the STIS PSF from the WN 8 star should be subtracted out with the background in the aperture extraction procedure. Furthermore, the centroid of the observed absorption trough is 8.9 Å over the Hα laboratory wavelength; this suggests that the line profile is significantly distorted as it is filled up with Hα emission arising in the wind. Finally, the overall shape of the Hα profile is very similar to that of other O If stars (e.g., Cygnus OB 7 and HD 210839, Herrero et al. 2000).

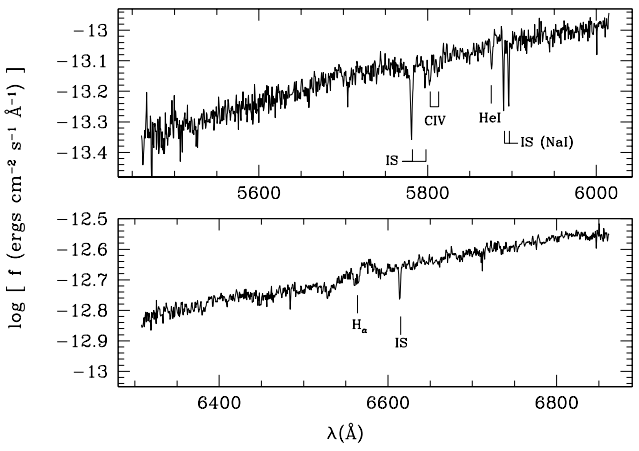

FIG. 9.—Line identification for the O star component in the WR 147 system. Well-defined intrinsic and interstellar absorption features are noted. Equivalent widths are listed in Table 6.

TABLE 6

LINE IDENTIFICATIONS IN THE SPECTRUM OF THE OB COMPONENT OF WR 147

ID	λ_{lab} (Å)	λ_{obs} (Å)	W_λ (Å)
C IV.....	5801.3	5802.5	0.40 ± 0.10
C IV.....	5811.9	5812.5	0.35 ± 0.10
He I.....	5875.6	5875.9	0.45 ± 0.10
Hα	6561.9	6570.8	-4.05 ± 0.05

This Hα emission suggests a substantial mass-loss rate, which would imply that the star is a supergiant in the Of category. However, C III λ5696 is not clearly in emission; this is more consistent with stars in the (f) category, which show a filling in of He II λ4686, but no strong emission lines. It is therefore not possible at this point to clearly distinguish between spectral class Ia, Iab, Ib, or II, but luminosity classes III–V can be excluded. We tentatively classify this star as O5–7 I–II(f).

4. DISCUSSION

4.1. *On the Absolute Magnitudes of the Components*

Absolute magnitudes M_v (in the narrowband photometric system defined by Westerlund 1966) have been estimated for Galactic WR stars on the basis of cluster and association membership (van der Hucht 2001, hereafter vdH01). The narrowband v is used because it avoids the brightest optical emission lines of WR stars. The distances of clusters and associations derived by Lündstrom & Stenholm (1984) are used. The mean absolute magnitudes M_v for WC 7, WC 6, and WN 8 stars are $M_v \simeq -4.5$, -3.5, and -5.5, respectively, with a standard deviation of $\lesssim 1.0$ mag.

The absolute magnitudes M_V of the OB stars can be estimated based on their spectral classification, using the relationships defined by SK82. While the v and V bands are not exactly the same, a comparison between V and v for a number of WR and OB stars shows that $|v-V| \lesssim 0.3$ (Westerlund 1966; see also Turner 1982). While the value of $v-V$ for any given WR star will be dependent on the strength of the optical lines, we can assume that $M_v \sim M_V$ to within less than half a magnitude.

We thus compare the difference in absolute magnitudes as determined from the spectral types with the measured difference in V derived using the WFPC2 images of these systems by Niemela et al. (1988). For the WR 86 system, the WC 7 star is expected be in the range $-5.5 < M_V < -3.5$, and SK82 quotes a value of $M_V \simeq -5.1$ for a B0 III star. The two estimates are thus consistent with each other, since the observed difference in V magnitude for this system is $V_{WR} - V_B = 0.02 \pm 0.18$.

For the WR 146 system, the WC 6 star is expected to be in the range $-4.5 < M_V < -2.5$, while SK82 quotes a mean value of $M_V \simeq -6.25$ for O8 I–II stars. The observed magnitude difference is $V_{WR} - V_B = -0.24 \pm 0.08$; there is thus a discrepancy of at least 2 mag between the observed magnitude difference and that inferred from the spectral types. The two stars are definitely companions, as evidenced by the confirmation of a colliding-wind region between the two components. The discrepancy thus cannot be

attributed to a chance alignment of two stars at different distances. If we assume that the O8 star is actually a main-sequence object (unlikely because of the Hα line in emission), we get $M_V = -5.15$ from SK82, which still yields a difference of at least 1 mag. This means either that the WR star is too bright for its spectral type or, alternately, that the O star is too faint. An intriguing comparison can be made between WR 146 and WR 86: both systems have components of approximately the same magnitude, but the WC 5 star in WR 146 is expected to be intrinsically fainter than the WC 7 star in WR 86, while the O8 I–II star in WR 146 is expected to be intrinsically brighter than the B0 III star in WR 86.

For the WR 147 system, the WN 8 star is expected to be in the range $-6.5 < M_V < -4.5$. From SK82 we get a range of values $-5.90 < M_V < -6.25$ for O5–7 stars with luminosity classes I–III. The observed magnitude difference is $V_{WR} - V_B = -2.16 \pm 0.12$. Again, we find that the WR component is too bright for its spectral type by at least 1.5 mag or, alternately, that the O star is too faint by at least 1.5 mag. To be consistent with the expected magnitude of a WN 8 star, the O star would have to be fainter than $M_V \approx -4.4$, which, in the SK82 tables, is only consistent with stars of type B0 or later. A spectral type of B is clearly ruled out by our STIS spectra.

Recently, absolute magnitudes of OB stars were reevaluated based on data by *Hipparcos* (Wegner 2000, hereafter W00). The values of M_V for giant and supergiant OB stars derived by W00 turn out to be fainter than the SK82 values by about 2 mag. Under the W00 system, the absolute magnitudes of WR 146 and WR 147 as estimated from the spectral types would be consistent with the observed magnitudes. Although the agreement is suggestive, one has to be concerned about the possible effects of the revised M_V from the W00 system on the distance to Galactic clusters and associations and hence on the absolute magnitudes derived by vdH01. One also has to consider the relatively large scatter in the absolute magnitudes of individual OB stars as derived from *Hipparcos* parallaxes. For O7–B0 stars, the scatter can be as large as ± 1 mag. There may also be systematic effects on parallax estimates of the OB star *Hipparcos* sample, especially since most of the OB stars are beyond 200 pc. Hence, the values derived from W00 must be used with caution.

Some of the discrepancy may arise because of the uncertainty in the determination of the spectral type of the OB components. In particular, the main criterion used in the determination of the luminosity class was the apparent filling in of the Hα line, which suggests high mass-loss rates in WR 146 and WR 147. However, both WR 146 and WR 147 are systems with colliding winds. If Hα emission arises in the shock front, this could fill up the Hα absorption line in the spectra of the OB companions, mimicking the effect of intense mass loss. If Hα emission arises near the head of the bow shock front, which is relatively close to the O star in both WR 146 and WR 147, then we would not be able to resolve them from the O star in the STIS data presented here, and this might explain the apparent filling in of the emission lines. On the other hand, if Hα emission were to arise downwind from the head of the bow shock, at some relatively large distance from both the WR and O components, then any extra Hα emission would appear as a diffuse component on the STIS data, which would not be strong enough (as we have shown from the lack of any detected diffuse emission; see § 2) to account for the apparent filling in of the emission lines.

4.2. *On the Binary Status and the Wind Collision*

The WR 146 and WR 147 systems exhibit strong nonthermal radio components. It has been found that the nonthermal emission occurs *between* the two stellar components, somewhat closer to the OB star (Dougherty et al. 1996; Williams et al. 1997). In the framework of the colliding-wind model developed by Eichler & Usov (1993), the shock front forms at a distance r_{OB} (r_{WR}) from the OB (WR) component. Given $D = r_{OB} + r_{WR}$ the distance between the two stars, then

$$r_{OB} = \frac{\eta^{1/2}}{1 + \eta^{1/2}} D \, , \tag{3}$$

where $\eta \equiv (\dot{M} v_\infty)_{OB}/(\dot{M} v_\infty)_{WR}$ is the wind momentum ratio. The ratio r_{OB}/D is dimensionless and independent of the projection of the system on the plane of the sky and thus can be measured directly from imaging.

For WR 146 and WR 147, $r_{OB}/D \simeq 0.25$ and 0.14, respectively, as measured directly from the combined radio maps and *HST* WFPC2 images (Niemela et al. 1998). These yield estimated values of $\eta = 0.10$ and $\eta = 0.028$ for WR 146 and WR 147, respectively. From the spectral types, we estimate that the O components in WR 146 and WR 147 have mass-loss rates $\dot{M}_O \sim 1\ 10^{-5}\ M_\odot\ \mathrm{yr}^{-1}$ (see Herrero et al. 2000). If we assume a typical terminal velocity $v_\infty \approx 2000$ km s^{-1} for the O stars (see Prinja, Barlow, & Howarth 1990), we can estimate the mass-loss rate of the WR components and check for consistency. For WR 146, taking $v_\infty = 2900$ km s^{-1} as the terminal velocity of the WC 6 star, this yields a mass-loss rate $\dot{M}_{WR} \sim 6.9\ 10^{-5}\ M_\odot\ \mathrm{yr}^{-1}$. This value is consistent with the mass-loss rate value of $\dot{M}_{WR} = 3.0 \pm 1.5\ 10^{-5}$ derived from the radio emission of the WR star by Dougherty et al. (1996). For WR 147, however, taking $v_\infty = 1100$ km s^{-1} as the terminal velocity of the WN 8 star (from Eenens & Williams 1994), one gets $\dot{M}_{WR} \sim 6.5 \times 10^{-4}\ M_\odot\ \mathrm{yr}^{-1}$, which is an order of magnitude larger than the mass-loss rate value of $\dot{M}_{WR} = 4.6\ 10^{-5}$ estimated from the radio emission by Williams et al. (1997).

For WR 147, Williams et al. (1997) have deduced a distance of ≈ 630 pc by comparing infrared photometry of WR 147 and WR 105, the latter being another WN 8 star suspected to be in the Sgr OB1 association, whose distance is known. It is from this estimated distance and from VLA measurements of the radio flux that Williams et al. (1997) have estimated the mass-loss rate in the WR component of WR 147 to be $4.2 \pm 0.2\ 10^{-5}\ M_\odot\ \mathrm{yr}^{-1}$. The disagreement with our estimated value can be resolved in two ways: (1) we have overestimated $\dot{M}_O$ by at least 1 order of magnitude, in which case the OB component in WR 147 is unlikely to be an O supergiant, or (2) WR 147 is more distant than estimated by Williams et al. (1997), i.e., at least 1 kpc away. If the latter interpretation is true, then there exist significant differences between the spectral energy distributions of WR 105 and WR 147. The former interpretation is more likely to be true, which means that we have overestimated the mass-loss rate of the O component because of an inaccurate assessment of the spectral type and luminosity class. The key element here is the observation of the filling in of the Hα profile, which does suggest a high mass-loss rate and luminosity. Clearly, a resolved spectrum of the OB component

in WR 147 spanning the whole optical range is required to resolve this issue. Such an observation will have to be performed with the *Hubble Space Telescope* or with similar high spatial resolution from the ground.

While WR 86 does show evidence for some nonthermal emission, it is listed by Dougherty & Williams (2000) as having a "composite" spectral energy distribution (as compared with a "nonthermal" spectral energy distribution for WR 146 and WR 147, and a "thermal" energy distribution for suspected single WR stars). We believe that the fact that this star has only a weak component of nonthermal emission can be explained by the smaller mass-loss rate from the B component. While late-Of stars typically have derived mass-loss rates $\dot{M} \sim 10^{-5}\ M_{\odot}\ \mathrm{yr}^{-1}$, a star of spectral type B0 III like the companion to WR 86 is expected to have a mass-loss rate $\sim 10^{-7}\ M_{\odot}\ \mathrm{yr}^{-1}$ or about 2 orders of magnitude smaller than Of stars (e.g., Runacres & Blomme 1996). Assuming V_{∞} for the B0 III star to be of the same order of magnitude as for the supergiant O stars in WR 146 and WR 147, this means that the wind momentum from the B0 III star must be 2 orders of magnitude smaller and r_{OB}, the distance from the OB star to the wind collision front, is expected to be 1 order of magnitude smaller for the WR 86 system than it is for WR 146 and WR 147. This means that the WR 86 shock front is formed much closer to the OB component and most likely wraps around the OB component with a much smaller opening angle. Hence, the total volume where nonthermal emission occurs should be significantly smaller, which accounts for the weaker nonthermal emission. This hypothesis can be tested by imaging the WR 86 system in the IR/radio at very high spatial resolution and locating the source of the weak nonthermal emission. We predict that the nonthermal emission occurs very close (a few milliarcseconds) to the OB component, where $r_{\mathrm{OB}}/D \sim 0.01$.

It has been suggested by Dougherty et al. (2000) that some apparent discrepancies in the luminosities of the components in WR 146 might be resolved if the O8 companion was itself a WR + O binary. Likewise, Setia Gunawan et al. (2000) have interpreted the observed 3.38 yr period in the 1.4 GHz radio emission as evidence for a third component in the system orbiting the O8 star. Our resolved spectra of WR 146 shows no clear evidence for a third component. It is true that the C IV emission feature in the O8 star spectrum, which we marked as contaminated light from the WC 6 star, does look significantly different from the actual C IV profile in the WC 6 spectrum, and thus one may argue that the so-called "contaminated light" could actually be the signature of another WR star orbiting the O8 component. We note, however, that (1) the fact that the PSF is strongly dependent on the wavelength most likely introduces a dependency on wavelength for the amount of contaminated light, which can distort the C IV profile on the O8 star, and (2) the extracted spectra being the result of a multidimensional fit of the whole double PSF profile, we do not necessarily expect the contamination to add up in a strictly linear fashion (i.e., effects may be nonlinear), which means that a disproportionately strong contamination could occur at the point where the C IV line is brightest, hence distorting the C IV profile in the O8 star spectrum. We therefore conclude that there is no evidence for another WR star orbiting the O8 star component on a tighter orbit. We can safely rule out the presence of any unresolved WR star, except for one that would be significantly fainter (at least 1 mag) than the resolved WC 6 component. Unless the WC 6 is unusually bright for its spectral type, this leaves only a relatively faint WR star of spectral type WC 3–WC 4 or WN 2–WN 3 (see van der Hucht 2001) as a possible (but unlikely) candidate. If the O8 star is an unresolved double, it is more likely to be an OB + OB system.

5. SUMMARY

We briefly summarize our findings as follows:

1. We have obtained resolved spectra of the components in the close visual binary systems WR 86, WR 146, and WR 147. WR 86 is classified as WC 7 + B0 III, with the WR component to the northwest and the B component to the southeast. WR 146 is classified as WC 6 + O8 I–IIf, with the WR component to the south and the O component to the north. WR 147 is classified as WN 8 + O5–7 I–II(f), with the WR component to the south and the O component to the north. The relative location of the WR and O components in the WR 146 and WR 147 systems is consistent with the colliding-wind interpretation of their radio maps.

2. Absolute magnitudes M_V of the OB stars have been derived, based on the spectral type–magnitude relationship of SK82 and compared with the estimated absolute magnitudes M_v of the Wolf-Rayet stars (from van der Hucht 2001). While the values are consistent for the WR 86 system, we find a significant discrepancy in the WR 146 and WR 147 systems. For WR 146 it looks as if the WC 6 star is at least 2 mag brighter than expected (or the O8 I–IIf star is at least 2 mag fainter than expected). For WR 147 the WN 8 star appears to be at least 1.5 mag brighter than expected [or the O5–7 I–II(f) star is fainter than expected].

3. From the spectral types, we estimate that the O components in WR 146 and WR 147 have mass-loss rates $\dot{M}_O \sim 10^{-5}\ M_{\odot}\ \mathrm{yr}^{-1}$. These values can be compared with the estimated values for the WR component mass-loss rate $\dot{M}_{\mathrm{WR}}$, which are linked to $\dot{M}_{\mathrm{O}}$ through the configuration of the colliding-wind systems. While the estimated value of $\dot{M}_{\mathrm{O}}$ for WR 146 is consistent with $\dot{M}_{\mathrm{WR}}$, our value of $\dot{M}_{\mathrm{O}}$ for WR 147 is an order of magnitude too large. This most likely indicates that our spectral classification is inaccurate, although it could also mean that current estimates of the distance to WR 147 are too low. A more accurate spectral classification for WR 147 is required to resolve the discrepancy, which will require new resolved spectroscopic observations of the OB component in WR 147.

4. From the spectral type, we estimate the B component in WR 86 to have $\dot{M} \sim 10^{-7}\ M_{\odot}\ \mathrm{yr}^{-1}$. The relatively smaller mass-loss rate in the OB component in WR 86 must result in the colliding-wind region being much smaller in volume and located much closer to the B star. Hence the amount of nonthermal emission arising in the shock cone is expected to be much smaller. The reduced mass-loss rate from the B star and smaller volume of the resulting shock cone explains why WR 86 is found to be a weak nonthermal emitter, while WR 146 and WR 147 are known strong nonthermal emitters.

5. In none of the systems did we observe any trace of diffuse emission down to the instrumental limit. If there is any diffuse emission in the optical associated with the colliding-wind interface, it must be weaker than 5×10^{-15} ergs $\mathrm{cm}^{-2}\ \mathrm{s}^{-1}\ \mathrm{\AA}^{-1}\ \mathrm{arcsec}^{-1}$.

Overall, we feel that the classification of OB stars, especially the determination of luminosity classes, is a difficult and nontrivial task. The main reason for this is the lack of availability of a uniform sequence of digital spectra spanning the whole spectral range from blue to red. Existing atlases, while useful, are sometimes fragmentary, and most are based on photographic spectra. Publication of a comprehensive atlas of digital spectra for OB stars based on CCD observations and covering the whole optical range from ~4000–7000 Å would be very beneficial to this field.

REFERENCES

Churchwell, E., Bieging, J. H., van der Hucht, K. A., Williams, P. M., Spoelstra, T. A. Th., & Abbott, D. C. 1992, ApJ, 393, 329
Conti, P. S. 1973, ApJ, 179, 181
———. 1976, Mem. Soc. R. Sci. Liège, 9, 193
Conti, P. S., & Alschuler, W. R. 1971, ApJ, 170, 325
Crowther, P., De Marco, O., & Barlow, M. J. 1998, MNRAS, 296, 367
Dougherty, S. M., & Williams, P. M. 2000, MNRAS, 319, 1005
Dougherty, S. M., Williams, P. M., & Pollacco, D. L. 2000, MNRAS, 316, 143
Dougherty, S. M., Williams, P. M., van der Hucht, K. A., Bode, M. F., & Davis, R. J. 1996, MNRAS, 280, 963
Eenens, P. R. J., & Williams, P. M. 1994, MNRAS, 269, 1082
Eichler, D., & Usov, V. 1993, ApJ, 402, 271
Hartkopf, W. I., Mason, B. D., Barry, D. J., McAlister, H. A., Bagnuolo, W. G., & Prietro, C. M. 1993, AJ, 106, 352
Herrero, A., Puls, J., & Villamariz, M. R. 2000, A&A, 354, 193
Jeffers, H. M., van de Bos, W. H., & Greeby, F. M. 1963, in Publ. Lick Obs., Index Catalog of Visual Double Stars (1961.0), 21, 1
Lündstrom, I., & Stenholm, B. 1984, A&AS, 58, 163
Massey, P., Conti, P. S., Niemela, V. S. 1981, ApJ, 246, 145
Milward, C. G., & Walker, G. A. H. 1985, ApJS, 57, 63
Moffat, A. F. J. 1969, A&A, 3, 455
———. 1995, IAU Symp. 163, Properties of Wolf-Rayet Binaries: The Key to Understanding Wolf-Rayet Stars (Dordrecht: Kluwer), 213
Moffat, A. F. J., Lamontagne, R., Shara, M. M., McAlister, H. A. 1986, AJ, 91, 1392
Niemela, V. S., Shara, M. M., Wallace, D. J., Zurek, D. R., & Moffat, A. F. J. 1998, AJ, 115, 2047
Prinja, R. K., Barlow, M. J., & Howarth, I. D. 1990, ApJ, 361, 607
Roberts, M. S. 1962, AJ, 67, 79
Runacres, M. C., & Blomme, R. 1996, A&A, 309, 544
Schmidt-Kaler, T. 1982, Landoldt-Bornstein, New Series, Group 6, Vol. 2b, Numerical Data Functional Relationships in Science and Technology, ed. K. Schaiffers & H. H. Voigt (Berlin: Springer), 1 (SK82)
Setia Gunawan, D. Y. A., van der Hucht, K. A., de Bruyn, A. G., & Williams, P. M. 2000, A&A, 356, 676
Smith, L. F. 1968, MNRAS, 138, 109
Smith, L. F., Shara, M. M., & Moffat, A. F. J. 1990, ApJ, 358, 229
———. 1996, MNRAS, 281, 163
Turner, D. G. 1982, in Wolf-Rayet Stars: Observations, Physics, Evolution (A82-48127 24-90) (Dordrecht: Reidel), 57
Tuthill, P. G., Monnier, J. D., & Danchi, W. C. 1999, Nature, 398, 487
van der Hucht, K. A. 1992, A&ARv, 4, 123
———. 2001, New A Rev., 45, 135 (vdH01)
van der Hucht, K. A., Conti, P. S., Lündstrom, I., & Stenholm, B. 1981, Space Sci. Rev., 28, 227
Walborn, N. R. 1980, ApJS, 44, 535
Walborn, N. R., & Fitzpatrick, E. L. 1990, PASP, 102, 379
Wallace, D. J., Gies, D. R., Nelan, E., & Leitherer, C. 2000, BAAS, 32, 97.04
Wegner, W. 2000, MNRAS, 319, 771 (2000)
Westerlund, B. E. 1966, ApJ, 145, 724
Williams, P. M. 1995, in ASP Conf. Ser. 93, Radio Emission from the Stars and the Sun, ed. A. R. Taylor & J. M. Paredes (San Francisco: ASP), 15
———. 1999, IAU Symp. 193, Wolf-Rayet Phenomena in Massive Stars and Starburst Galaxies, ed. K. A. van der Hucht, G. Koenigsberger, & P. R. J. Eenens (San Francisco: ASP), 267
Williams, P. M., Dougherty, S. M., Davis, R. J., van der Hucht, K. A., Bode, M. F., & Setia Gunawan, D. Y. 1997, MNRAS, 289, 10